Chemical Geology 441 (2016) 35–46

Contents lists available at ScienceDirect

Chemical Geology

journal homepage: www.elsevier.com/locate/chemgeo

Trace elements (Li, B, Mn and Ba) as sensitive indicators for salinization and freshening events in coastal aquifers

A. Russak [a,b,*], O. Sivan [a], Y. Yechieli [b,c]

[a] Department of Geological and Environmental Sciences, Ben Gurion University of the Negev, Beer Sheva, P.O.B 653, Beer-Sheva, 84105, Israel
[b] Geological Survey of Israel, Malkei Israel St. 30, Jerusalem, 95501, Israel
[c] Department of Environmental Hydrology & Microbiology, Zuckerberg Institute for Water Research, Blaustein Institutes for Desert Studies, Ben Gurion University of the Negev, Sede Boqer, 8499000, Israel

ARTICLE INFO

Article history:
Received 11 March 2016
Received in revised form 29 July 2016
Accepted 3 August 2016
Available online 05 August 2016

Keywords:
Seawater intrusion
Fresh-saline water interface
Trace metal
Manganese
Lithium
Boron

ABSTRACT

The current global intrusion of seawater into coastal aquifers causes salinization of groundwater and thus significant degradation of its quality. This study quantified the effect of seawater intrusion and freshening events in coastal aquifers on trace elements (Li, B, Mn and Ba) across the fresh-saline water interface (FSI) and their possible use as indicators for these events. This was done by combining field data and column experiments simulating these events. The experiments enabled quantification of the processes affecting the trace element composition and examination of whether salinization and freshening events are geochemically reversible, which has been seldom investigated.

The dominant process affecting trace element composition during salinization and freshening is ion exchange. The results of the experiments show that the concentrations of major cations and Li^+ were reversible during salinization and freshening, whereas B, Mn^{2+} and Ba^{2+} were not. During salinization, Li^+ and B were depleted due to sorption by 10 and 100 $\mu mol \cdot L^{-1}$, respectively, to about half of their expected conservative concentrations. The relative depletion of Li^+ increased with distance from the shore, representing the propagation of salinization. Ba^{2+} and Mn^{2+} were desorbed from the sediment during salinization and enriched by tenfold in the aqueous phase compared to their concentration in seawater (~0.1 $\mu eq \cdot L^{-1}$). During freshening both were depleted by almost tenfold compared to their concentration in fresh groundwater (~0.7 $\mu eq \cdot L^{-1}$). The depletion of Mn^{2+} is a sensitive marker for freshening because Mn^{2+} has a strong affinity to the solid phase. Moreover, this study shows that both Mn^{2+} and Ba^{2+} can be used as sensitive hydrogeochemical tools to distinguish between salinization and freshening events in the FSI zone in coastal aquifers.

1. Introduction

1.1. Salinization and freshening events

Seawater intrusion is defined as the migration of salt water from the sea into a fresh water aquifer (Freeze and Cherry, 1979), and is one of the main causes for the degradation of groundwater quality in coastal aquifers. The transition zone between the salt water and fresh groundwater is known as the fresh-saline water interface (FSI). Salinization due to seawater intrusion can be defined as the movement of the FSI toward the land. Freshening is the inverse event during which the aquifer is flushed by fresh water. It can be defined as the repulsion of the FSI toward the sea. Quantifying the effect of salinization and freshening on the chemical composition of the water is important for management of coastal fresh groundwater. The severe shortage in water in many coastal areas is expected to cause farther over-pumping and thus movement of the FSI inland. This is an important issue especially due to expected global climate change which can cause a decrease in recharge and a rise in sea level. This may result in elevated FSI in various locations, depending on several factors such as topography (e.g., Yechieli et al., 2010).

One of the important factors in aquifer management is the reversibility of processes occurring as a result of seawater intrusion. Whether salinization and freshening events are reversible from the hydrological point of view is debatable (e.g., Werner et al., 2013). It is clear that contamination of coastal aquifers due to seawater intrusion evolves quickly, while freshening of aquifers by flushing of fresh groundwater takes a longer period of time (e.g., Adorni-Braccesi et al., 2000; Foster and Chilton, 2003). A good example for studying seawater-intrusion reversibility is the study of seawater intrusion in Israel. Intense salinization of the central area of the coastal aquifer in Israel (Tel-Aviv) occurred between 1934 and 1948 (Zilberbrand et al., 2001). Thus, pumping was reduced in 1959 and fresh water was injected into the aquifer in 1964, but the FSI was not pushed seawards (Mandel and Goldenberg, 1986).

* Corresponding author at: Department of Geological and Environmental Sciences, Ben Gurion University of the Negev, Beer Sheva, P.O.B 653, Beer-Sheva, 84105, Israel.
E-mail addresses: russak@bgumail.bgu.ac.il (A. Russak), oritsi@bgu.ac.il (O. Sivan).

http://dx.doi.org/10.1016/j.chemgeo.2016.08.003
0009-2541/

However, in 1999 it was noted that the FSI retreated in some areas in the coastal aquifer of Israel (including Tel-Aviv) (Melloul and Zeitoun, 1999).

The main known geochemical effect of seawater intrusion into coastal aquifers (salinization) and flushing of the aquifer (freshening) is cation exchange, which is the sorption and desorption of cations on and from the sediment of the aquifer (e.g., Andersen et al., 2005; Appelo et al., 1990; Jones et al., 1999; Russak and Sivan, 2010; Valocchi et al., 1981). If the amount of sorption or desorption during salinization of a certain cation is equal to the amount of the inverse process during freshening, this indicated the geochemical reversibility of salinization and freshening. One of the objectives of this study is to evaluate the geochemical reversibility of salinization and freshening events.

1.2. Trace elements in the FSI

Recent studies have shown that trace elements are affected by ion exchange during salinization and freshening events. During seawater intrusion dissolved Li^+ and boron (B) are depleted due to sorption (Jones et al., 1999). On the other hand, during freshening dissolved Li^+ is enriched (Stuyfzand, 1992). Other studies showed that the dissolved B concentration increases during freshening (Ravenscroft and McArthur, 2004) and decreases during salinization (Faye et al., 2005).

Cation exchange is also suggested to be the dominant process controlling the changes of Fe^{2+}, Mn^{2+} and Ba^{2+} during seawater intrusion and freshening events in the Netherlands (Stuyfzand, 1992). Fe^{2+}, Mn^{2+} and Ba^{2+} ions were mobilized during seawater intrusion, whereas during freshening the concentrations of dissolved Mn^{2+} and Fe^{2+} declined (Stuyfzand, 1992). For Fe^{2+} and Mn^{2+} enrichment, dissolution of minerals such as siderite ($FeCO_3$) and rhodochrosite ($MnCO_3$) was suggested as an explanation. Barite ($BaSO_4$) dissolution was excluded as a possible explanation for Ba^{2+} enrichment because the North Sea water is supersaturated with respect to barite (Stuyfzand, 1992). Changes in Fe^{2+} and Mn^{2+} at or below the FSI were also attributed to redox reactions (Charette et al., 2005; Windom et al., 2006). Fe^{2+} and Mn^{2+} were later oxidized when the saline groundwater moved upward (Charette et al., 2005). A similar phenomenon was observed in soil aquifer treatment (SAT), where under suboxic conditions manganese oxides were reduced and when groundwater reached oxic conditions, Mn^{2+} was sorbed on aquifer sediments (Oren et al., 2007). Using column experiments, it was concluded that sorption of Mn^{2+} mostly controls the fate of Mn^{2+}, although up to 20% of the removed Mn^{2+} was via precipitation as $MnCO_3$ (Goren et al., 2012).

Barium enrichment in saline water in the Hudson estuary was also explained by cation exchange (Li and Chan, 1979). Other studies found high concentrations of Ba^{2+} in saline groundwater and deduced that this occurred due to cation exchange (Charette and Sholkovitz, 2006; Shaw et al., 1998). Interestingly, authors of these studies noticed that the enrichment is most clearly observed in the mixing zone. Furthermore, in Brazil (Patos-Mirim Lagon area) the groundwater is enriched with Ba^{2+} as well, and the explanation for that was desorption and dissolution of minerals (Windom and Niencheski, 2003). Mn^{2+} oxide dissolution under anoxic condition was suggested to release Ba^{2+} to groundwater (Charette et al., 2005; Charette and Sholkovitz, 2006). It was concluded that the aquifer acts as a Ba^{2+} sink for fresh groundwater and as a source for saline waters and that saline groundwater can supply Ba^{2+} to coastal oceans (Moore, 1999).

The main objective of this research was to examine the potential use of the trace elements – Li, B, Mn and Ba – as indicators for distinguishing between salinization and freshening events. This was tested by combining field work and column experiments simulating salinization and freshening events. The controlled conditions in the experiments – salinization/freshening regime, known and constant water velocity, known natural end members' composition, known pore volume and continuous sampling - enabled quantification of the processes occurring during salinization and freshening.

2. Methods

2.1. Study site and field sampling

The study area was the coastal aquifer of Israel, which is located along the eastern Mediterranean coastline. The aquifer's geological section consists of alternating layers of calcareous sandstone (Kurkar), red loam (Hamra), and marine clays of Pleistocene age (Issar, 1968), which overlie impervious marine clays of Pliocene age (the Saqiye Group). The field work was conducted in the Nizzanim Nature Reserve (Nizzanim) that is located near Ashdod (Fig. 1). Groundwater samples were collected from a set of monitoring wells that were located perpendicular to the shore line (112b, 112S and 112 W) at different distances from the shore (40, 70 and 220 m, respectively) (Fig. 1).

The field samplings were conducted at the end of the summer, the dry season (September 2011) and in the winter, the rainy season (January 2012). Samples from borehole 112b were taken using thin tubing (3 mm I.D., 40 m) mounted on a peristaltic pump. The volume of the tube (500 mL) was pumped and removed prior to collecting a sample. The depth of the water table in 112S and 112 W was more than 10 m, thus, these boreholes were sampled by a submersible pump (Grundfos). One volume of the tube (about 5 L) was pumped and removed before sampling. Sampling began only after the electrical conductivity (EC) had reached stable values. A seawater sample from the shore area near 112b was taken in January 2012. Major ions, Br^-, Li^+ and B were analyzed from the same subsample. Subsamples for trace metals (Fe^{2+}, Mn^{2+} and Ba^{2+}) were acidified by nitric acid (0.1 N final concentrations). All samples were kept refrigerated (4 °C) until analyses.

2.2. Laboratory experiments

A column experiment (10 cm I.D., 30 cm) was conducted using aquifer sediments, fresh groundwater and seawater taken from the Nizzanim area. The sediment represents the Israeli Coastal Aquifer: calcareous sand, consisting almost 90 wt.% quartz (0.7–0.9 mm sized), 10 wt.% calcium carbonate, 0.5 wt.% clay and 0.5 wt.% organic matter. The sediment was packed slowly by depositing small amounts of the original sand sample (with no prior drying) by spoon into thin layers (~1 cm) of water.

The experiment was conducted under anaerobic conditions to simulate the natural conditions in the saline groundwater. It was maintained by purging N_2 gas, which contained an atmospheric level of CO_2 (~300 ppmv), into the water tank (fresh groundwater or seawater). The CO_2 was used in order to replace the original dissolved CO_2 that had been removed from the water due to the purging. A peristaltic pump was used to keep a flow rate of about 1 $mL{\cdot}min^{-1}$ from the water tank through the column. The water was flowing from the column through a small vial (~5 mL), designed for constantly monitoring the DO level by using DO electrode, and than the water flowed out through the tubes to be sampled. The experiment lasted for about a month.

The experiment simulated seawater intrusion (salinization) by replacing fresh groundwater by seawater and then flushing the seawater by fresh groundwater (freshening). The column was flushed by fresh water before the salinization part of experiment was conducted in order to ensure that the pore water in the column was saturated with the experimental fresh groundwater end-member. It should be noted that fresh groundwater for the experiment was taken in two sampling campaigns. The concentration of Mn^{2+} was different between the first and second end-members (0.5 and 0.8 $\mu eq{\cdot}L^{-1}$, respectively). More detailed information about the experimental design is found in Russak et al. (2015a).

2.3. Examination of the reversibility of cation exchange during salinization and freshening

In order to determine if the salinization cycle is reversible, the amount of cations sorbed and desorbed during salinization should be

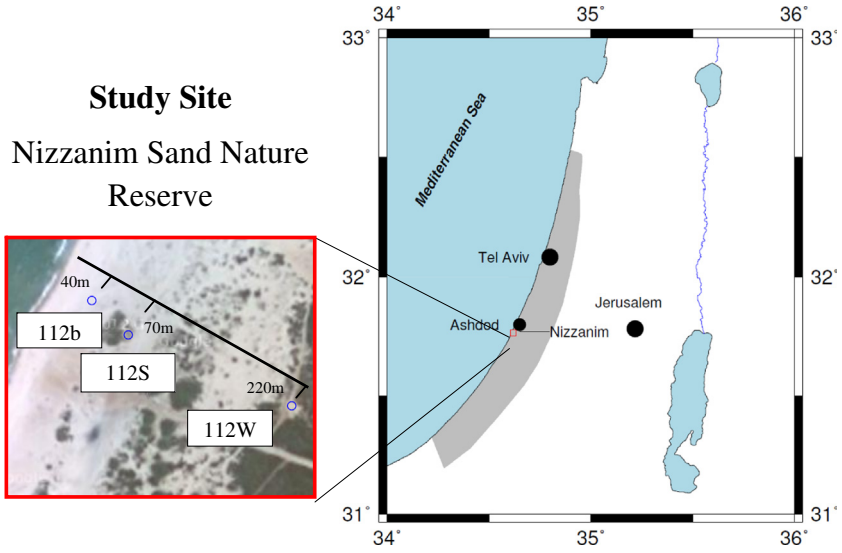

Fig. 1. Map of the coastal aquifer of Israel (in gray) and detailed map (modified from http://amudanan.co.il) of the study site (Nizzanim) with the location of the monitoring wells (112b, 112S and 112 W) that located perpendicular to the shore line.

calculated and compared with the amount of cations sorbed and desorbed during freshening. The mass balance of the different cations was conducted by calculating the area between the breakthrough curve of measured concentrations during the column experiments (salinization or freshening) and that of a calculated theoretical concentration which would be expected from the conservative behavior of each specific cation. The expected value was calculated using the Cl^- concentration as a reference for a conservative ion. First, the seawater fraction (f_{sw}) of a sample point from the experiment was determined using the concentration of Cl^- of the sample (Cl_i) and of the end members - fresh groundwater (Cl_{fw}) and seawater (Cl_{sw}) - used in the experiment, as follows (Appelo and Postma, 1999):

$$f_{sw} = (Cl_i - Cl_{fw})/(Cl_{sw} - Cl_{fw}) \quad (1)$$

The expected value of the cation (M_{expc}) was then calculated using the f_{sw} and the concentration of this cation in the end members – fresh groundwater and seawater (M_{fw} and M_{sw}, respectively), as follows (Appelo and Postma, 1999):

$$M_{expc} = f_{sw} \times M_{sw} + (1 - f_{sw}) \times M_{fw} \quad (2)$$

Plotting the breakthrough curves of the measured and the expected cation together reveals the deviation of the cation from conservative behavior. If the measured concentration was below the expected concentration, then the cation was depleted (sorbed) and if it was above the expected, then it was enriched (desorbed). The breakthrough curve of Ca^{2+} is a good example for this because its depletion and enrichment are clear (Fig. 2, the area of sorption and desorption marked in green).

The area between the measured and the expected concentrations is estimated by calculating the area between two sequential sampling points on the breakthrough curve of the measured and expected cation, using the formula for a trapezoid area:

$$\text{Area} = \text{height} \times (\text{sum of bases})/2 \quad (3)$$

The height is the difference of pore volumes between the two sampling points. The bases are the concentration of the cation at each point. The difference between the trapezoid areas of measured and expected breakthrough curve results is the amount of cation desorbed or sorbed (if the area has a negative value). The sum of all these areas gives the total amount of cation sorbed or desorbed during the experiments (salinization or freshening). The result of the trapezoid area is in units of meq per L times the number of pore volumes, thus in order to reach meq units, the volume of the pore water of the column of each experiment (in L units) is multiplied.

The calculation was made for the salinization experiment followed by the freshening experiment. For the major cations (Na^+, K^+, Mg^{2+}, Ca^{2+}) and Sr^{2+} the calculations were made for four experiments, two with a large column (pore volumes of 850 mL; Russak et al., 2015a) and two with a smaller column (pore volumes of 100 mL; Russak and

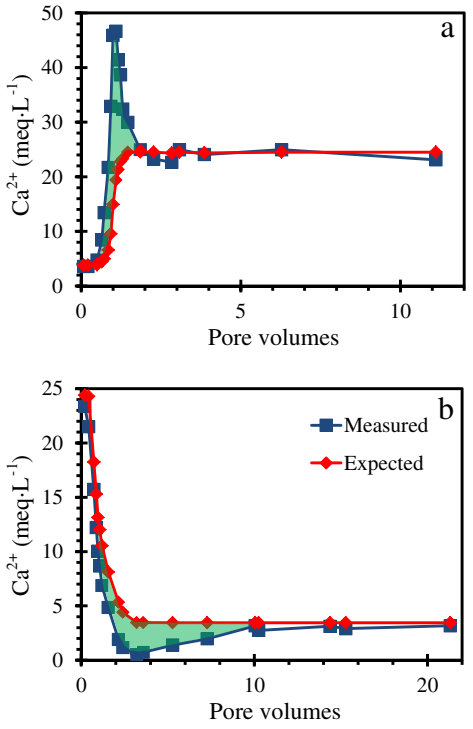

Fig. 2. Measured and expected from conservative behavior breakthrough curves of Ca^{2+} from salinization (a) and freshening (b). The areas of enrichment (due to desorption) during salinization and depletion (due to sorption) during freshening are marked in green. (For interpretation of the references to colour in this figure legend, the reader is referred to the web version of this article.)

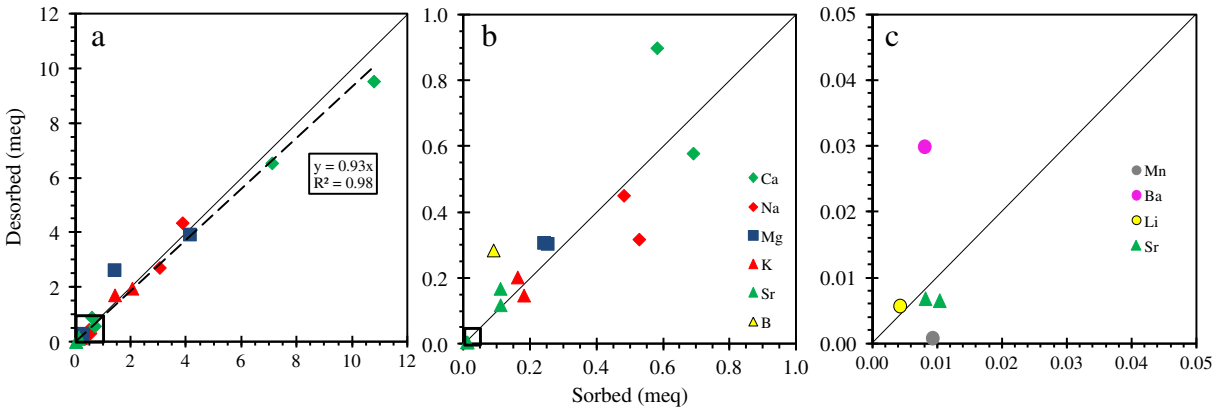

Fig. 3. The amount (in units of meq) of the desorbed ions versus sorbed ions due to ion exchange during salinization and freshening experiments (including data from Russak and Sivan, 2010) – Ca^{2+} (green rhombus), Na^{+} (red rhombus), Mg^{2+} (blue square), K^{+} (red triangle), Sr^{2+} (green triangle), B (yellow triangle), Mn^{2+} (gray circle), Ba^{2+} (pink circle) and Li^{+} (yellow circle) (a). (b) is a zoom in on (a) and (c) is a zoom in on (b). The black dashed line represents the trend line and the thin line represents line of a slope of 1. Note that there is one legend for all the graphs in the figure. (For interpretation of the references to colour in this figure legend, the reader is referred to the web version of this article.)

Sivan, 2010). For the trace elements Li^{+}, B, Mn^{2+} and Ba^{2+} the calculations were made only for one experiment using the larger column.

2.4. Analytical methods

Major cations, SO_4^{2-}, Fe^{2+}, Mn^{2+} and Ba^{2+} concentrations were analyzed by inductively coupled plasma-atomic emission spectroscopy (ICP-AES, P-E optima 3300) with a precision of 2% for the majors and 5% for the trace metals. Br^{-}, Li^{+} and B were analyzed by inductively coupled plasma-mass spectrometry (ICP-MS, Elan DRC II, Perkin Elmer) with a precision of 5%. Cl^{-} was measured by titration with 0.01 N $AgNO_3$ solution, and low Cl^{-} concentration (below 100 meq·L^{-1}) samples were analyzed by ion chromatography (Dionex 4000i). The errors calculated by averaging duplicate samples in both methods were less than 3%. Total alkalinity (ALK) was measured by titration (785 DMP Titrino, Metrohm) with 0.01 N HCl. The error calculated by averaging duplicate samples was ±0.03 mmol·L^{-1}.

The stable isotope composition of sulfur in sulfate ($\delta^{34}Sso_4$) was determined as described by Antler et al. (2013). SO_4^{2-} was precipitated as barium sulfate (barite) by adding a saturated barium chloride solution. The barite was combusted in a Flash Element Analyzer, resulting in sulfur dioxide (SO_2) which was measured by GS-IRMS (Thermo, Delta V

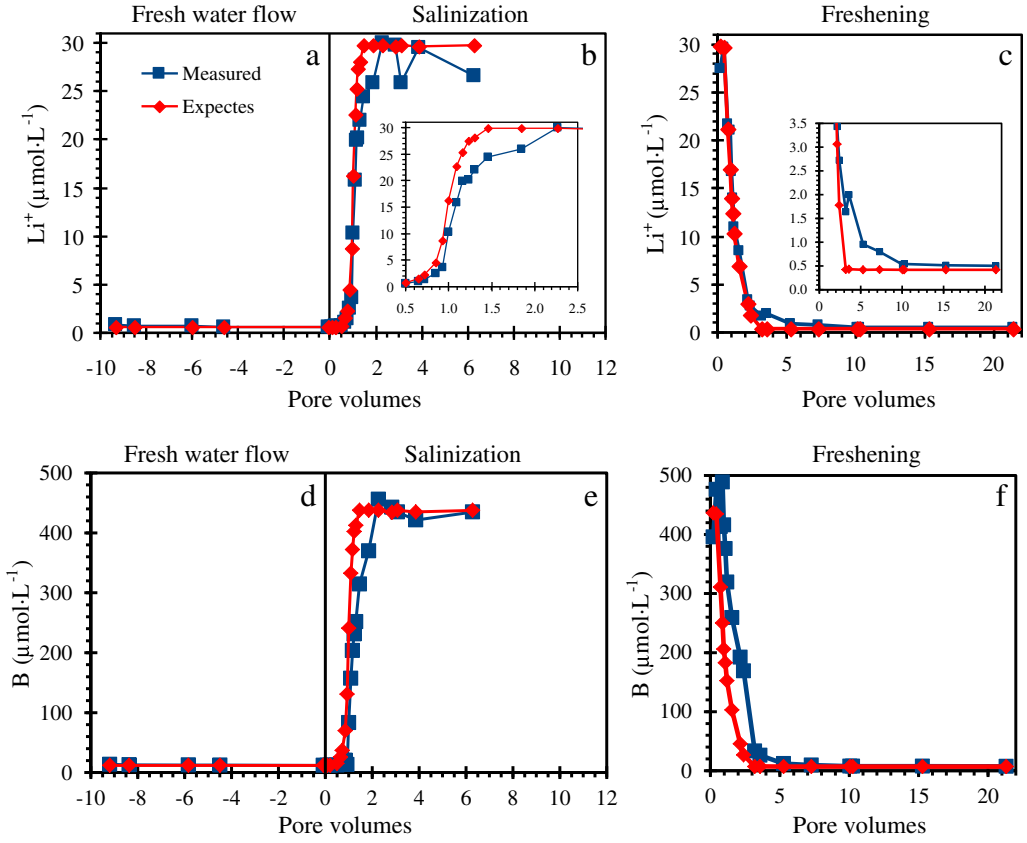

Fig. 4. Breakthrough curves of measured and expected concentrations from conservative behavior of Li^{+} and B during fresh water flow before salinization experiment (a and d), salinization experiment (b and e) and freshening experiment (c and f). The Li^{+} and B are depleted during salinization and enriched during freshening. Note that zoom-in of the salinization and freshening graphs of Li^{+} are displayed. The legend appears on one graph but refers to all the graphs in the figure.

Plus). The error was determined from the standard deviation between duplicates (between 0.2 and 0.4‰).

3. Results

In order to determine if the exchange process is reversible with the shifting of the events over the temporal scale of these experiments, the amount of desorbed versus sorbed ions during the salinization and freshening experiments was calculated (Fig. 3). The trend line calculated from the experiments for all ions (best fit) is 0.93 (Fig. 3a) with R^2 of 0.98. The results show that the major cations (Fig. 3a and b), Sr^{2+} (Fig. 3b and c) and Li^+ (Fig. 3c) fall on a line with a slope of 1, meaning full reversibility, while the trace elements B (Fig. 3b), Mn^{2+} and Ba^{2+} (Fig. 3c) are not equally sorbed and desorbed.

To examine the chemical behavior of the trace elements during the experiments we used breakthrough curves, which present trace element concentration versus time (as pore volume). The breakthrough curves of Li^+, B, Mn^{2+} and Ba^{2+} are displayed in Figs. 4a-c, d-f, 5a-c and d-f, respectively. During the salinization experiment, the measured concentration of Li^+ was lower than the expected concentration from simple mixing and conservative behavior (Fig. 4b). For example, after 1.46 pore volumes the concentration of Li^+ was 24 μmol·L^{-1}, while the expected concentration from conservative behavior was expected to reach the concentration of Li^+ in seawater – 30 μmol·L^{-1}. However, the Li^+ concentration reached seawater concentration only after 2.27 pore volumes. The zoom-in of the salinization graph (detail graph of Fig. 4b) shows that the measured concentration of Li^+ had a lower concentration than expected: at 0.93 pore volumes the measured concentration was 3.7 μmol·L^{-1}, while the expected concentration was 8.7 μmol·L^{-1}. During freshening, the concentration of Li^+ was higher than expected, but only in the detail graph is clearly shown that its concentration was enriched (its concentration was higher than expected from conservative behavior) from 2.4 to 10 pore volumes. For example, at 5.28 pore volumes the measured concentration was 1.0 μmol·L^{-1}, while the expected concentration was 0.4 μmol·L^{-1}. Similarly, B had a lower concentration than expected from conservative behavior during salinization (Fig. 4e). At 1.46 pore volumes, B concentration was only 315 μmol·L^{-1}, lower than the expected conservative concentration of 438 μmol·L^{-1}. However, during freshening the B concentration was higher than expected from mixing and for a longer time than Li^+ — from 0.73 to 10 pore volumes (Fig. 4f).

Mn^{2+} and Ba^{2+} had higher dissolved concentrations than expected from conservative behavior during the salinization experiment and concentrations below the conservative concentration during the freshening experiment (Fig. 5). The Mn^{2+} and Ba^{2+} concentrations reached their peaks at the same time – after 1.09 pore volumes. At this point, the Mn^{2+} concentration was higher by a factor of 5 and Ba^{2+} by a factor of 80 than the expected conservative concentrations (Fig. 5e and f, respectively). During freshening, the Mn^{2+} and Ba^{2+} concentrations were much below their expected concentrations. However, Mn^{2+} reached its minimum concentration before Ba^{2+}, at 0.43 pore volumes as compared to 2.4 for Ba^{2+}. The minimum concentration of Mn^{2+} during freshening was less than 0.07 meq·L^{-1}, which is the detection limit for Mn^{2+} (Fig. 5c). For Ba^{2+} it was 0.06 meq·L^{-1} (Fig. 5f).

To compare field data to the experimental data, Br^-, K^+, Li^+ and B were displayed versus Cl^-. It can be seen that all the samples of Br^- plotted on the mixing line between fresh water and seawater (Fig. 6a). On the other hand, the K^+ concentration was below the mixing line during salinization and above it during freshening (Fig. 6b). Li^+ (Fig. 6c) and B (Fig. 6d) showed non-conservative behavior, similar to K^+.

The set of observation wells, perpendicular to the shore line, was used to get a better perception of the system by enabling to display 2D view of the FSI zone and the fresh and saline groundwater adjacent

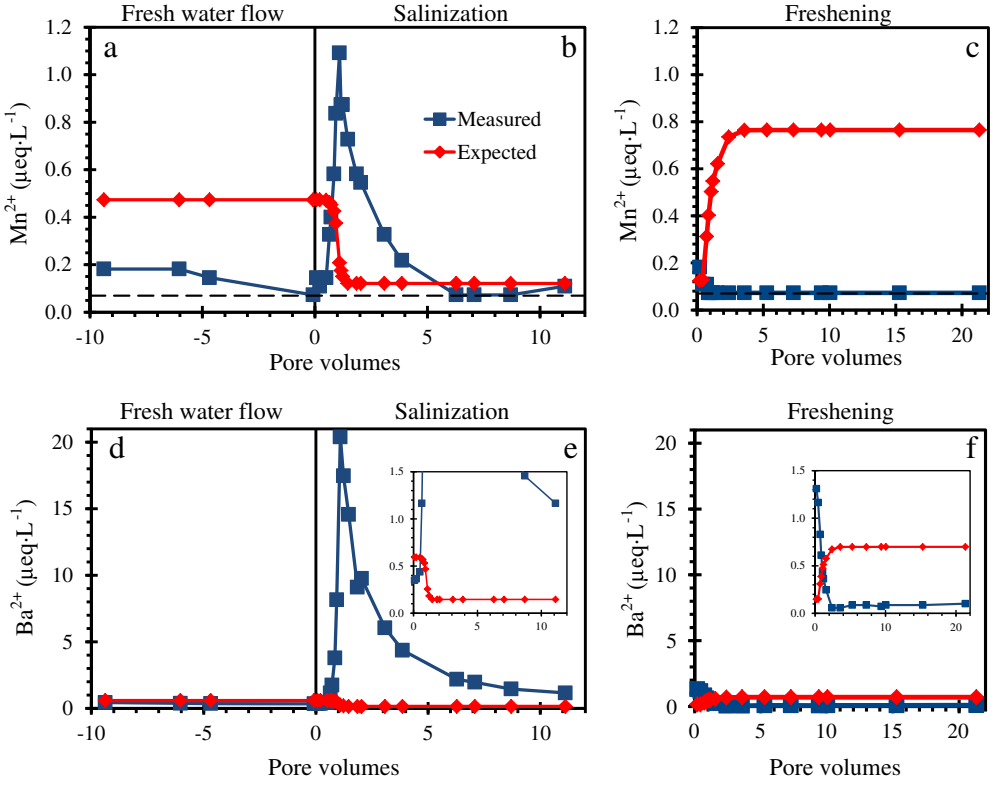

Fig. 5. Breakthrough curves of measured and expected concentrations from conservative behavior of Mn^{2+} and Ba^{2+} during fresh water flow before salinization experiment (a and d), salinization experiment (b and e) and freshening experiment (c and f), respectively. The Mn^{2+} and Ba^{2+} are enriched during salinization and depleted during freshening. The black dashed line denote the detection limit (D.L.) of Mn^{2+} (0.07 μeq·L^{-1}). Note that zoom-in of the salinization and freshening graph of Ba^{2+} are displayed. The legend appears on one graph but refers to all the graphs in the figure.

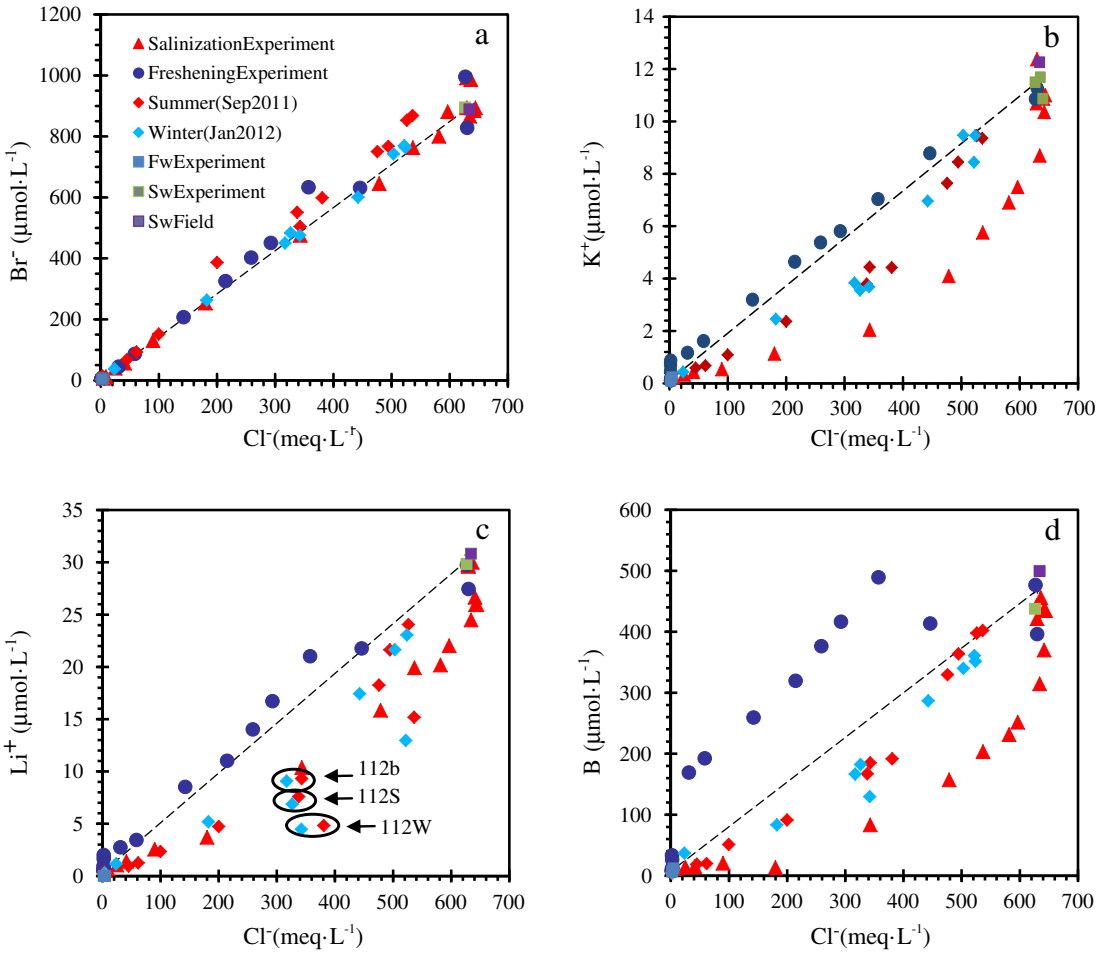

Fig. 6. Br^- (a), K^+ (b), Li^+ (c) and B (d) versus Cl^- of data obtained from the salinization (red triangle) and freshening (blue circle) experiments and field data from summer (red rhombus) and winter (blue rhombus). Black dashed line represents the mixing line between fresh water (FW, blue square) and seawater (SW) from experiment (green square) and field (purple square). Br^- is a conservative species, while B and Li^+ are non-conservative. Black circles mark the points representing the different observation wells. Note that Li^+ concentration is depleted in the same order as the distance of the wells from shore. The legend appears on one graph but refers to all the graphs in the figure. (For interpretation of the references to colour in this figure legend, the reader is referred to the web version of this article.)

it. The 2D view of Cl^- shows distinctly the location of the FSI zone and that there is no significant difference between summer and winter (Fig. 7). To show the effect of the chemical processes in the FSI zone, the Ca^{2+} data is given as the deviation between the measured and expected (by mixing only) Ca^{2+} concentration (ΔCa). The higher ΔCa is in the FSI zone, up to 20 meq·L^{-1} (dark green, Fig. 8). The values of Mn^{2+} and Ba^{2+} concentrations are given without comparison to the expected values, because there is only a slight difference between their concentrations in fresh groundwater and seawater (the end-members). The highest Mn^{2+} concentration in summer was 9.1 meq·L^{-1}, and in winter it was 0.51 meq·L^{-1} in the well located most inland (112 W, Fig. 9). The Ba^{2+} concentration in the FSI zone in well 112 W was high in the summer – 2-3 meq·L^{-1}, while in winter its concentration in the FSI zone was only 0.7 meq·L^{-1} (Fig. 10). Ba^{2+} concentration was also higher in the shallow depths of the well located in the inter-tidal zone (112b), reaching a peak of 5.7 meq·L^{-1} in the summer.

4. Discussion

Major cations in the FSI were previously shown to be affected mainly by ion exchange process, and can be used as a salinization index (e.g., Stuyfzand, 2008; Russak and Sivan, 2010). We aimed here to quantify the processes affecting trace element concentrations in the FSI and to test whether trace elements can provide a more sensitive indicator to salinization/freshening events as potential new tools for identification of seawater intrusion.

4.1. The reversibility of cation exchange process during salinization and freshening

The reversibility of the cation exchange processes can be tested by plotting the same ion on a desorbed/sorbed graph. The average slope of the total sorbed versus desorbed major ions during the experiments is 0.93, implying that salinization and freshening events are geochemically reversible (Fig. 3a). This means that after a shift between salinization and freshening, the aquifer returns to the original state of sorption and the cation exchange process can repeat in the next cycle of salinization and freshening. Cycles of salinization/freshening may explain why measured concentrations of cations in the FSI show deviations from conservative behavior even if the seawater intrusion began a long time ago and has not reached seawater concentration. For example, in Israel the latest seawater intrusion began about 30 years ago, but the cation exchange process is affecting the major cations today in a similar way as 15 years ago. In other words, the trends of the major ions, like Ca^{2+}, with regard to the mixing line were similar 15 years ago (Sivan et al., 2005) to the trends today. Therefore, it seems that the reversibility is not seasonal because the saline groundwater is deviated from seawater for all those years and does not reach the composition of the end member (seawater).

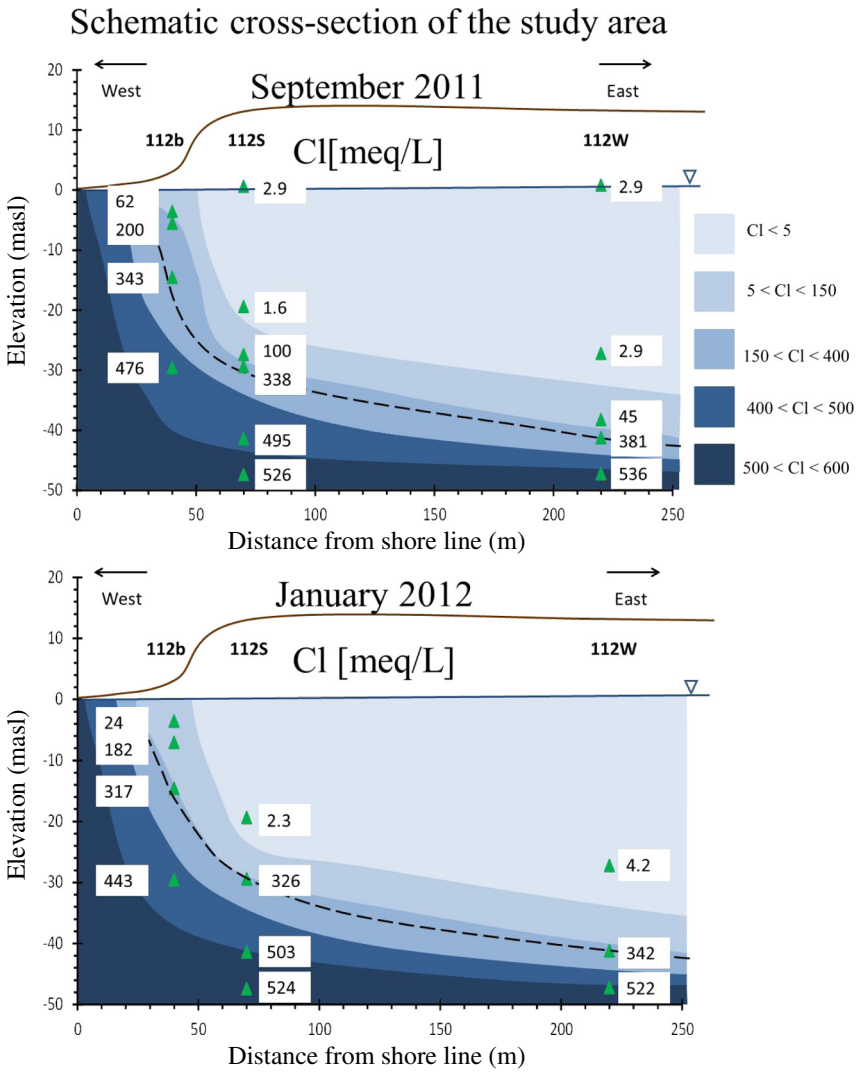

Fig. 7. Schematic cross section showing Cl^- concentration in 2D view from the field in summer (September 2011) and winter (January 2012). Green triangles represent the sampling points. The different areas (in different shade of blue) represent range of values to emphasize the FSI zone. The dashed line represent salinity of about half of the salinity in seawater. Note that the FSI zone in summer and winter located in the same area. (For interpretation of the references to colour in this figure legend, the reader is referred to the web version of this article.)

The cation exchange process during a freshening experiment is not a mirror image of the cation exchange process during a salinization experiment. During salinization, the cation exchange process affects the cation concentrations more significantly than during the freshening experiment. However, the cation exchange process during the salinization experiment is more rapid than during the freshening. In other words, during salinization, each ion is affected dramatically and quickly by the exchange process and during freshening the effect is relatively milder but continues for a longer time. Therefore the amount of ions desorbed/sorbed during the salinization experiment is similar to the amount of ions sorbed/desorbed during freshening (Fig. 3).

Regarding boron, its concentration deviated from the expected conservative behavior by more than 100 $\mu mol \cdot L^{-1}$ (Fig. 4e and f). It is interesting to note that during salinization this effect continued only for about 0.6 pore volumes, whereas during freshening B was enriched strongly for 1.7 pore volumes. Therefore, the amount of B desorbed from the sediment during freshening was three times larger than that sorbed during salinization (Fig. 3b).

Manganese was enriched during salinization and depleted during freshening (Fig. 5b, c), quite similar to the behavior of Ca^{2+} (Fig. 2). In general, Mn^{2+} exhibits a great affinity to being sorbed and its concentration during freshening decreased below the detection limit (0.07 $\mu eq \cdot L^{-1}$) from the beginning of the experiment up to its end (0.8–21.3 pore volumes). During salinization, the Mn^{2+} reached the seawater concentration. Therefore, the amount of Mn^{2+} that desorbed during salinization is 10 times smaller than the amount of Mn^{2+} that was sorbed during freshening (Fig. 3c). Another evidence for the tendency of Mn^{2+} to be sorbed was displayed during the fresh water flow, before the salinization experiment, when the Mn^{2+} concentration decreased below the concentration of Mn^{2+} in the fresh water entering the column. The strong affinity of Mn^{2+} to be sorbed under a fresh water regime was also described in previous laboratory studies (e.g., Oren et al., 2007; Goren et al., 2012). It should be noted that this experiment was done under anoxic conditions, so it is not likely that Mn-oxides precipitated. Moreover, it seems that rhodochrosite ($MnCO_3$) could not precipitate during this part of the experiment. It is impossible to support this by the measurement of bicarbonate (HCO_3^-) since the concentration of HCO_3^- is in the range of few $mmol \cdot L^{-1}$, whereas the Mn^{2+} concentration is in the range of only 1 $\mu mol \cdot L^{-1}$. However, calculation of the saturation index (SI) using PHREEQC (Parkhurst and Appelo, 1999) show that the water was under-saturation with respect to rhodochrosite – (SI for rhodochrosite was in the range of −0.5 to −1.5). Thus, the behavior of Mn^{2+} in the salinization-freshening cycle is irreversible and it accumulates on the sediment during these processes.

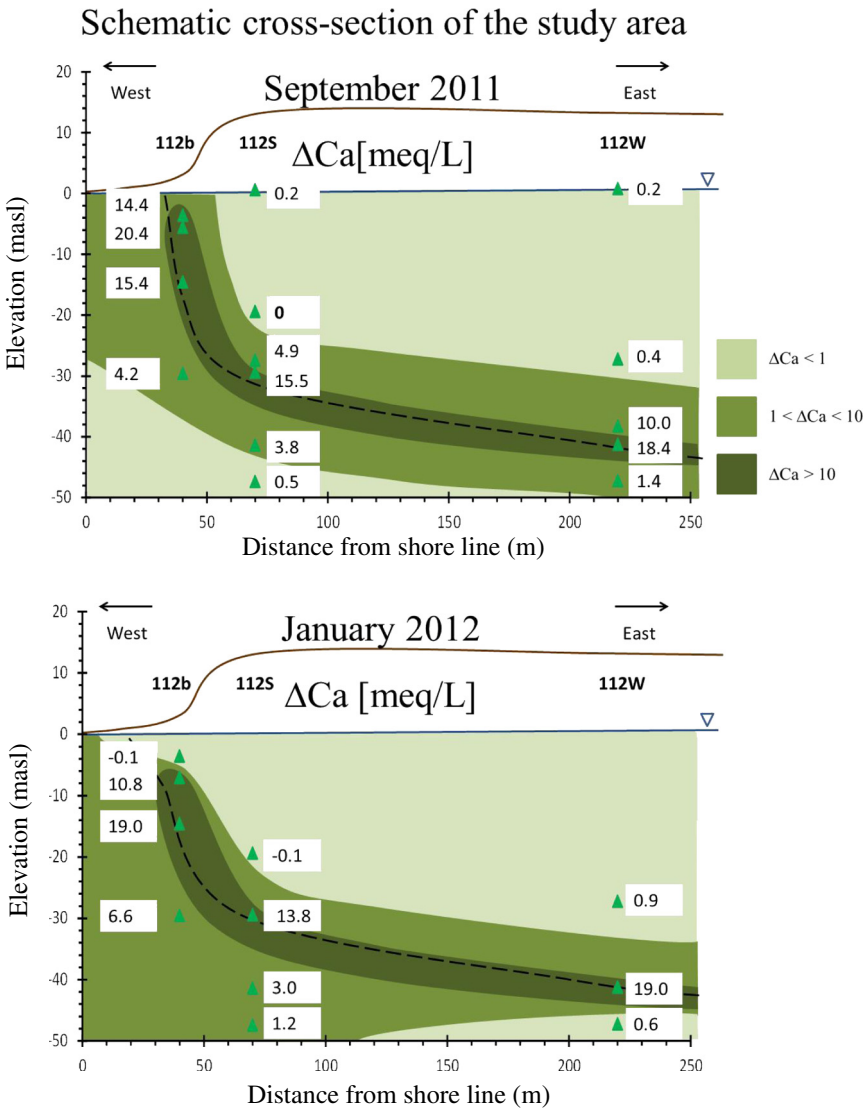

Fig. 8. Schematic cross section showing ΔCa (difference between measured and expected from mixing) in 2D view from the field in summer (September 2011) and winter (January 2012). Green triangles represent the sampling points. The different areas (in different shade of green) represent range of values to emphasize the area of the enrichment of Ca^{2+}. The dashed line represent salinity of about half of the salinity in seawater. The Ca^{2+} enriched mostly in the FSI area. Note that there is slight different between summer and winter. (For interpretation of the references to colour in this figure legend, the reader is referred to the web version of this article.)

The amount of Ba^{2+} that was desorbed during salinization is three times larger than the depleted amount during freshening (Fig. 3c). However, Ba^{2+} did not reach the concentration of the end-members and theoretically, if the salinization and freshening continued for longer time, the amount of sorption and desorption would have been different. It seems that the sorption processes may continue longer than the experiment time, because the line of the measured concentration and the expected concentration are parallel lines (Fig. 5f). On the other hand, the desorption process nearly finished because the line of the measured concentration shows a tendency to decrease, approaching the values of the expected concentration of the end member (Fig. 5e). Therefore, it seems that the salinization-freshening cycle of Ba^{2+} is irreversible. Nevertheless, it should be noted that dissolution of barite minerals during salinization and/or precipitation during freshening is not likely to affect the Ba^{2+} as was deduced by calculation of the SI. During salinization, when Ba^{2+} was enriched, the SI for barite was in the range of 0.5 to 1, meaning that the water was over-saturated with respect to barite. During freshening, Ba^{2+} was depleted and the SI for barite was −0.6, meaning that the water was under saturated with respect to barite.

It is hard to deduce an absolute time scale of the reversibility process from the laboratory experiments since the time scale is expressed in pore volumes (PVs). However, the experiments provide an indication of the relative timescale to reach the saline end member and the fresh end member. In these terms, it is clear that the salinization is faster than freshening (e.g., 2 PVs and 10PVs for Ca^{2+}, respectively). To implement this on the field it is necessary to estimate what is the "pore volume" in the field (if it is the aquifer, the FSI or just the area where there are oscillation in the FSI due to salinization and freshening etc.). It seems that the salinization and freshening cycle is seasonal (Russak et al., 2015b), which is probably not enough for full reversibility.

4.2. Trace elements in the FSI

The major ions Ca^{2+} and K^{+} can be used as proxies to distinguish between salinization and freshening (Russak and Sivan, 2010). The similarity of the general trend generated by the trace elements and by Ca^{2+} and K^{+} suggested that they should be examined as proxies as well. The experiments exhibit a clear difference between the effect of salinization and freshening on these cations.

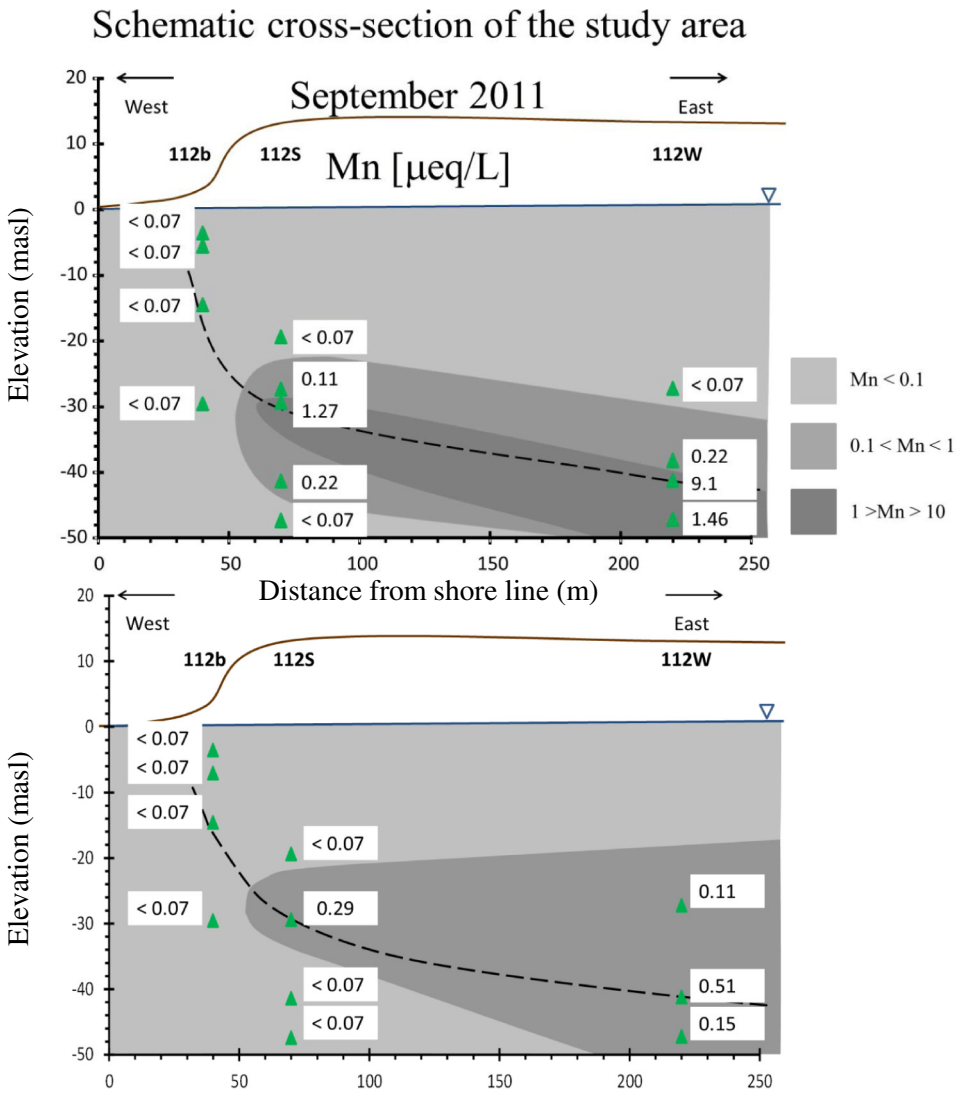

Fig. 9. Schematic cross section showing Mn^{2+} concentration in 2D view from the field in summer (September 2011) and winter (January 2012). Green triangles represent the sampling points. The different areas (in different shade of gray) represent range of values to emphasize the change in Mn^{2+} concentration. The dashed line represent salinity of about half of the salinity in seawater. Note that Mn^{2+} reached to a very high concentrations in the FSI zone inland and to a much higher concentration in summer than in winter. (For interpretation of the references to colour in this figure legend, the reader is referred to the web version of this article.)

On the other hand, Br^- can be referred to as a conservative species based on the current study, and in agreement with previous studies (e.g., Sivan et al., 2005). Li^+ behaves like K^+, showing depletion during salinization; thus, like K^+, it can be used as evidence for salinization. Moreover, the Li^+ concentration is less depleted in the observation well closest to the shore (observation well 112b) than in the farther well (observation well 112 W), which implies that the process of cation exchange during seawater intrusion (salinization) continues while the seawater intrudes farther inland.

Boron also shows depletion during salinization (Fig. 6d), like K^+ and Li^+. This phenomenon can be an advantage in desalination of saline groundwater compared to desalination of seawater because the removal of B during reverse osmosis (RO) is relatively limited (e.g., Gorenflo et al., 2007; Kloppmann et al., 2008). This is significant because the potential for desalination of saline groundwater over seawater has been recently shown (e.g., Stein et al., 2016).

The 2D cross section of Cl^- content shows that the FSI is located approximately in the same place in summer and winter (dashed line in Fig. 7). The Cl^- can be used as a reference for the location of the FSI, but it does not identify the process occurred in the FSI – salinization or freshening. For that other indicators are needed. The Ca^{2+} concentration in seawater is higher than in fresh water, thus the enrichment in Ca^{2+} is shown by ΔCa - the calculated difference between the measured and expected from the mixing concentration. In summer and winter, the ΔCa is high in the FSI zone in a similar way (Fig. 8), which implies that seawater intrusion (salinization) also occurs in this area during winter. On the other hand, the values of Mn^{2+} in the FSI in summer are higher than in winter, implying that more seawater intrusion occurs during the summer (Fig. 9). This means that Mn^{2+} is affected by freshening and that it can be used as a more sensitive indicator for the early stage of freshening, while Ca^{2+} only indicates when the freshening was completed. Moreover, the maximum concentration of Mn^{2+} exhibited in the observation well located most inland (112 W) implies that the cation exchange occurs with the seawater intrusion even at distance of more than 200 m. The FSI results of Ba^{2+} in the 112 W also show a decrease in winter compared to summer (Fig. 10), which suggests that the effect of freshening began there.

The results of this study show that Mn^{2+}, Ba^{2+} and Li^+ are affected strongly by cation exchange due to salinization and freshening, and thus can be used as hydrogeochemical tools to identify salinization processes in the FSI zone in coastal aquifers. Moreover, these tracers are more sensitive than Ca^{2+} and K^+. Mn^{2+} and Li^+ (Figs. 6c and 9, respectively)

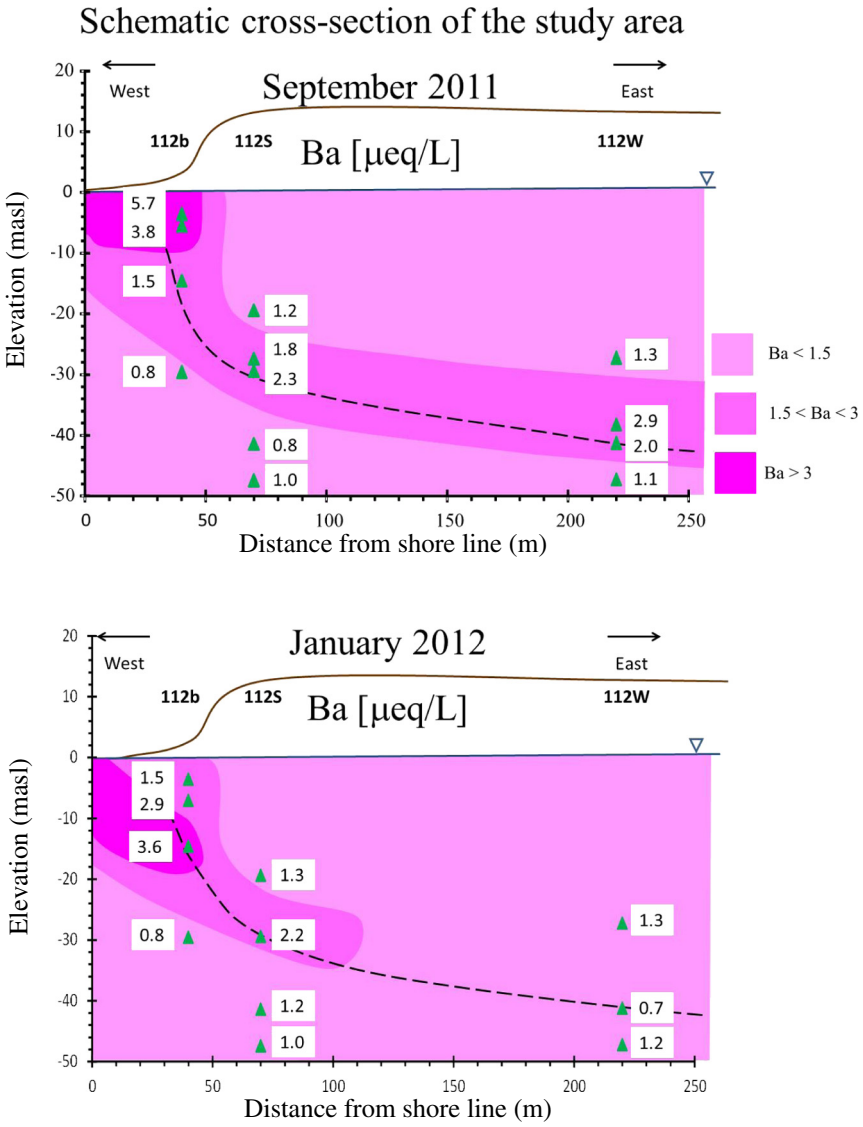

Fig. 10. Schematic cross section showing Ba^{2+} concentration in 2D view from the field in summer (September 2011) and winter (January 2012). Green triangles represent the sampling points. The different areas (in different shade of pink) represent range of values to emphasize the change in Ba^{2+} concentration. The dashed line represent salinity of about half of the salinity in seawater. Note that Ba^{2+} reached to its maximum concentration under the beach area (well 112b) and in summer reached to higher concentration than in winter. (For interpretation of the references to colour in this figure legend, the reader is referred to the web version of this article.)

were more affected at the sample points located landward. This implies that the salinization front propagated landward and thus the salinization effect (cation exchange) is more significant. Li^{+} shows this phenomenon (more depletion in the boreholes further inland) in summer and in winter at the same magnitude. However, Mn^{2+} shows a clear difference between summer and winter, indicating that the salinization is more dominant in summer than in winter. The strong affinity of Mn^{2+} to be sorbed may explain why the seasonal variation is better exhibited in Mn^{2+} values than in the Li^{+} values.

The enrichment of Ba^{2+} in the FSI zone showed a slight seasonal variation, like Mn^{2+}. However, the maximum enrichment of Ba^{2+} was displayed in observation well 112b, which is located near the shore line. Moreover, in summer the maximum concentration was in the shallow depth, while in winter the maximum concentration was deeper (Fig. 10). This means that the salinization not only derived from the seawater intrusion into the aquifer below the FSI, but also from infiltration from above during flooding of the sea, probably during intense sea storms. Evidence for a sea storm in mid-August 2011 was given by wave data from the Israel Meteorological Service and data of the water-table head from *in situ* sensors in observation well 112 W (Levanon et al., 2013). The results of Ba^{2+} a month later (September 2011) and five months later (January 2012) showed how the groundwater below the area of the inter-tidal zone was affected and changed in time.

High concentrations of Fe^{2+} and Mn^{2+} in groundwater in the vicinity of the sea were explained by the process of reduction of Fe-oxides and Mn-oxides (Charette and Sholkovitz, 2006; Windom et al., 2006). Contamination of Mn^{2+} as a result of reduction of Mn-oxides was found in soil aquifer treatment of sewage reclamation (Oren et al., 2007). The high concentration of dissolved organic carbon (DOC) in the treated sewage was explained as the cause for the reductive conditions. In the present study site, the DOC concentrations were low, in the range of seawater (0.2 mM and even lower; Table A1.2 in Appendix A). Furthermore, sulfate (SO_4^{2-}) and the stable isotope ratio in SO_4^{2-} ($\delta^{34}S_{SO4}$) in a few samples in the experiments (salinization and freshening) and from the summer sampling campaign are plotted on the mixing line (Fig. 11a and b, respectively), indicating that sulfate was not used for bacterial respiration, as it behaves as a conservative species and not show any fractionation enrichment (Antler et al., 2013). Therefore, it is not reasonable to assume that anaerobic sulfate reduction

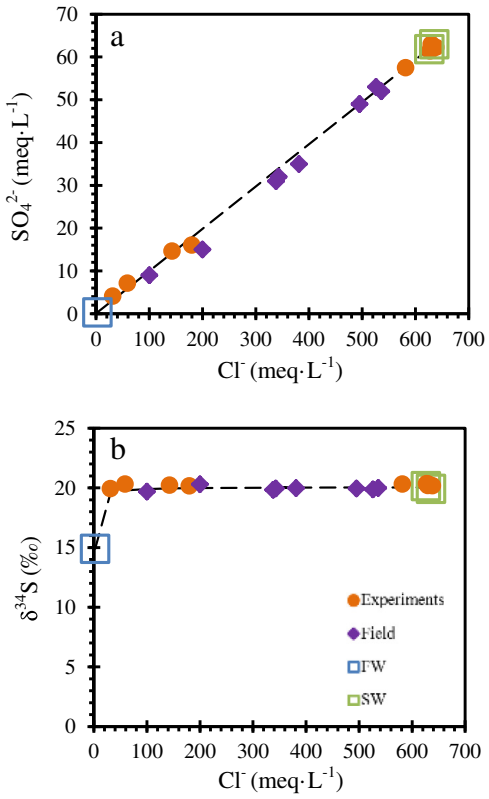

Fig. 11. SO_4^{2-} (a) and $\delta^{34}S_{SO4}$ (b) versus Cl^- from the experiments (salinization and freshening, orange circle), field (summer, purple rhombus). Black dashed line represents the mixing between fresh water (FW, open blue square) and seawater (SW, open green square). The results are plotted on the mixing line, indicating that SO_4^{2-} is a conservative parameter, thus there is no anaerobic reduction of SO_4^{2-}. The legend appears on one graph but refers to all the graphs in the figure. (For interpretation of the references to colour in this figure legend, the reader is referred to the web version of this article.)

occurred. Moreover, Fe^{2+} results from the experiments and field are below the detection limit (0.4 μeq·L^{-1}, Table A3 in Appendix A), indicating that Fe^{2+} was not significantly affected by biological reduction of ferric oxides to Fe^{2+}. These observations suggest that Mn^{2+} (like SO_4^{2-} and Fe^{2+}) was not affected significantly by anaerobic microbial respiration, and that the dominant process influencing Mn^{2+} concentrations in the aquifer is cation exchange.

5. Summary and Conclusions

This study examined the effects of salinization and freshening events in coastal aquifers on trace metals (Li^+, B, Mn^{2+} and Ba^{2+}) by combining field results and column experiments simulating these events. The major cations and the trace metals were mainly affected by cation exchange. The experiments suggest that circulation of salinization and freshening is reversible for the major cations (Na^+, K^+, Ca^{2+} and Mg^{2+}) including Sr^{2+} and Li^+, i.e., the amount of sorption or desorption of each cation due to exchange during salinization is almost equal to the amount desorbed or sorbed during freshening. On the other hand, B, Mn^{2+} and Ba^{2+} seem to have an irreversible behavior, as their concentrations did not revert to their original ones after the shifting between salinization and freshening.

The trace elements, Li^+, Mn^{2+} and Ba^{2+} are good indicators for identifying salinization and freshening events. Major cations show only the dominant situation in the aquifer (after salinization or after freshening), whereas Li^+ and Mn^{2+} also show the propagation of the seawater intrusion. This is because there is an increasing effect of cation exchange on Li^+ and Mn^{2+} with increased distance from the shore line. Ba^{2+} was the most enriched in the samples from the observation well in the inter-tidal zone (the nearest to shore), implying that Ba^{2+} could be used as a hydrogeochemical tool for identifying salinization due to intense sea storms.

Acknowledgements

We thank H. Hemo, S. Ashkenazi, H. Lutzky, I. Swaed and E. Levanon from the Israeli Geological Survey for their help in the field. We also thank O. Yoffe, G. Sharabi and D. Stiber from the Israeli Geological Survey and G. Antler and A.V. Turchyn from the University of Cambridge (UK), for their help with sample analyses. This research was supported by the Israel Science Foundation (OS #857/09) and the Israel Water Authority (OS and YY).

Appendix A. Supplementary data

Supplementary data to this article can be found online at http://dx.doi.org/10.1016/j.chemgeo.2016.08.003.

References

Adorni-Braccesi, A., Sciuto, P.F., Caboi, R., Cidu, R., Cristini, A., Fanfani, L., Rundeddu, L., Zuddas, P., 2000. Effect of sea water intrusion on Hg-mobilization in coastal aquifers: The case of Monte Argentario (Italy). In: Nriagu, J. (Ed.), Proceedings of the International Conference on Heavy Metals in the Environment. Ann-Arbor, MI. Elsvier Science Publisher, Oxford, U. K.

Andersen, M.S., Nyvang, V., Jakobsen, R., Postma, D., 2005. Geochemical processes and solute transport at the seawater/freshwater interface of a sandy aquifer. Geochim. Cosmochim. Acta 69, 3979–3994.

Antler, G., Turchyn, A.V., Rennie, V., Herut, B., Sivan, O., 2013. Coupled sulfur and oxygen isotope insight into bacterial sulfate reduction in the natural environment. Geochim. Cosmochim. Acta 118, 98–117.

Appelo, C.A.J., Postma, D., 1999. Ion exchange and sorption. Geochemistry, Groundwater and Pollution. A.A. Balkema, Rotterdam, the Netherlands, pp. 142–198.

Appelo, C.A.J., Willemsen, A., Beekman, H.E., G.J., 1990. Geochemical calculations and observations on salt water intrusions II. validations of geochemical model with laboratory experiments. J. Hydrol. 120, 225–250.

Charette, M.A., Sholkovitz, E.R., 2006. Trace element cycling in a subterranean estuary: Part 2. Geochemistry of the pore water. Geochim. Cosmochim. Acta 70, 811–826.

Charette, M.A., Sholkovitz, E.R., Hansel, C.M., 2005. Trace element cycling in a subterranean estuary: Part 1. Geochemistry of the permeable sediments. Geochim. Cosmochim. Acta 69, 2095–2109.

Faye, S., Maloszewski, P., Stichler, W., Trimborn, P., Faye, S.C., Gaye, C.B., 2005. Groundwater salinization in the Saloum (Senegal) delta aquifer: minor elements and isotopic indicators. Sci. Total Environ. 343, 243–259.

Foster, S.S.D., Chilton, P.J., 2003. Groundwater: the processes and global significance of aquifer degradation. Philos. Trans. R. Soc. Lond. Ser. B Biol. Sci. 358, 1957–1972.

Freeze, R.A., Cherry, J.A., 1979. Groundwater. Prentice-Hall, Inc., Englewood Cliffs, N.J.

Goren, O., Lazar, B., Burg, A., Gavrieli, I., 2012. Mobilization and retardation of reduced manganese in sandy aquifers: Column experiments, modeling and implications. Geochim. Cosmochim. Acta 96, 259–271.

Gorenflo, A., Brusilovsky, M., Faigon, M., Liberman, B., 2007. High pH operation in seawater reverse osmosis permeate: First results from the world's largest SWRO plant in Ashkelon. Desalination 203 (1), 82–90.

Issar, A., 1968. Geology of the central coastal plain of Israel. Isr. J. Earth Sci. 17, 16–29.

Jones, B.F., Vengosh, A., Rosenthal, E., Yechieli, Y., 1999. Geochemical Investigations. In: Bear, J., Cheng, A.-D., Sorek, S., Ouazar, D., Herrera, I. (Eds.), Seawater Intrusion in Coastal Aquifers — Concepts. Kluwer Academic Publications, Methods and Practices, pp. 51–71.

Kloppmann, W., Vengosh, A., Guerrot, C., Millot, R., Pankratov, I., 2008. Isotope and ion selectivity in reverse osmosis desalination: geochemical tracers for man-made freshwater. Environ. Sci. Technol. 42 (13), 4723–4731.

Levanon, E., Yechieli, Y., Shalev, E., Friedman, V., Gvirtzman, H., 2013. Reliable monitoring of the transition zone between fresh and saline waters in coastal groundwater. Groundw. Monit. Remediat. 33, 101–110.

Li, Y.H., Chan, L.H., 1979. Desorption of Ba and ^{226}Ra from river-borne sediments in the Hudson estuary. Earth Planet. Sci. Lett. 43, 343–350.

Mandel, S., Goldenberg, L.C., 1986. Anomalies of seawater-intrusion and seawater- repulsion in the area of Tel Aviv. Conjuctive Water Use (Proceedings of the Budapest Symposium). IAHS Publ. no. 156, pp. 241–248.

Melloul, A.J., Zeitoun, D.G., 1999. A semi-empirical approach to intrusion monitoring in Israeli coastal aquifer. In: Bear, J., Cheng, A.H.D., Sorek, S., Ouazar, D., Herrera, I. (Eds.), Seawater Intrusion in Coastal Aquifers — Concepts, Methods and Practices. Kluwer Academic Publications, pp. 543–558.

Moore, W.S., 1999. The subterranean estuary: a reaction zone of ground water and sea water. Mar. Chem. 65, 111–125.

Oren, O., Gavrieli, I., Burg, A., Guttman, J., Lazar, B., 2007. Manganese mobilization and enrichment during soil aquifer treatment (SAT) of effluents, the Dan Region Sewage Reclamation Project (Shafdan), Israel. Environ. Sci. Technol. 41, 766–772.

Parkhurst, D.L., Appelo, C.A.J., 1999. User's guide to PHREEQC (Version 2): A computer program for speciation, batch-reaction, one-dimensional transport, and inverse geochemical calculation.
Ravenscroft, P., McArthur, J.M., 2004. Mechanism of regional enrichment of groundwater by boron: the examples of Bangladesh and Michigan, USA. Appl. Geochem. 19, 1413–1430.
Russak, A., Sivan, O., 2010. Hydrogeochemical tool to identify salinization or freshening of coastal aquifers determined from combined field work, experiments, and modeling. Environ. Sci. Technol. 44, 4096–4102.
Russak, A., Sivan, O., Herut, B., Lazar, B., Yechieli, Y., 2015a. The effect of salinization and freshening events in coastal aquifers on nutrient characteristics as deduced from column experiments under aerobic and anaerobic conditions. J. Hydrol. 529, 1282–1292.
Russak, A., Yechieli, Y., Herut, B., Lazar, B., Sivan, O., 2015b. The effect of salinization and freshening events in coastal aquifers on nutrient characteristics as deduced from field data. J. Hydrol. 529, 1293–1301.
Shaw, T.J., Moore, W.S., Kloepfer, J., Sochaski, M.A., 1998. The flux of barium to the coastal waters of the southeastern USA : The importance of submarine groundwater discharge. Geochim. Cosmochim. Acta 62, 3047–3054.
Sivan, O., Yechieli, Y., Herut, B., Lazar, B., 2005. Geochemical evolution and timescale of seawater intrusion into the coastal aquifer of Israel. Geochim. Cosmochim. Acta 69, 579–592.
Stein, S., Russak, A., Sivan, O., Yechieli, Y., Rahav, E., Oren, Y., Kasher, R., 2016. Saline groundwater from coastal aquifers as a source for desalination. Environ. Sci. Technol. 50, 1955–1963.
Stuyfzand, P.J., 1992. Behaviour of major constituents in fresh and salt intrusion waters, in the Western Netherlands. In: Custodio, E. (Ed.), Study and Modeling of Salt Water Intrusion into Aquifers, Proc. 12th Salt Water Intrusion Meeting. CIHS-CINME, Barcelona, pp. 143–160.
Stuyfzand, P.J., 2008. Base exchange indices as indicators of salinization or freshening of (Coastal) Aquifers. Proceedings of the 20th Salt Water Intrusion Meeting, Naples, FL, June 23–27; Program and Proceedings Book, pp. 262–265.
Valocchi, A.J., Street, R.L., Roberts, P.V., 1981. Transport of ion-exchanging solutes in groundwater: Chromatographic theory and field simulation. Water Resour. Res. 17, 1517–1527.
Werner, A.D., Bakker, M., Post, V.E.A., Vandenbohede, A., Lu, C., Ataie-Ashtiani, B., Simmons, C.T., Barry, D.A., 2013. Seawater intrusion processes, investigation and management: Recent advances and future challenges. Adv. Water Resour. 51, 3–26.
Windom, H., Niencheski, F., 2003. Biogeochemical processes in a freshwater–seawater mixing zone in permeable sediments along the coast of Southern Brazil. Mar. Chem. 83, 121–130.
Windom, H.L., Moore, W.S., Niencheski, L.F.H., Jahnke, R.A., 2006. Submarine groundwater discharge: A large, previously unrecognized source of dissolved iron to the South Atlantic Ocean. Mar. Chem. 102, 252–266.
Yechieli, Y., Shalev, E., Wollman, S., Kiro, Y., Kafri, U., 2010. Response of the Mediterranean and Dead Sea coastal aquifers to sea level variation. Water Resour. Res. 46, W12550.
Zilberbrand, M., Rosenthal, E., Shachnai, E., 2001. Impact of urbanization on hydrochemical evolution of groundwater and on unsaturated-zone gas composition in the coastal city of Tel Aviv, Israel. J. Contam. Hydrol. 50, 175–208.